Evidence that SARS-CoV-2 Induces Lung-Cell Senescence: Potential Impact on COVID-19 Lung Disease

Larissa Lipskaia, Pauline Maisonnasse, Charles Fouillade, Valentin Sencio, Quentin Pascal, Jean-Michel Flaman, Emmanuelle Born, Arturo London-Vallejo, Roger Le Grand, David Bernard, et al.

HAL Id: hal-03395181

https://hal.sorbonne-universite.fr/hal-03395181

Submitted on 22 Oct 2021

Evidence that SARS-CoV-2 Induces Lung-Cell Senescence: Potential Impact on COVID-19 Lung Disease

Larissa Lipskaia, PhD[1,2], Pauline Maisonnasse, PhD[3], Charles Fouillade, PhD[4], Valentin Sencio, PhD[5], Quentin Pascal, PhD[3], Jean-Michel Flaman, PhD[6], Emmanuelle Born, [1], Arturo London-Vallejo, PhD[4], Roger Le Grand, PhD[3], David Bernard, PhD[6], François Trottein, PhD[5,*], Serge Adnot, MD, PhD[1,2,7 co-corr*]

[1]Univ Paris Est Creteil, INSERM U955, IMRB, F-94010 Créteil, France

[2]AP-HP, Hôpital Henri Mondor, Département de Physiologie-Explorations Fonctionnelles, and FHU Senec, F-94010, Créteil, France

[3]Center for Immunology of Viral, Auto-immune, Hematological and Bacterial diseases (IMVA-HB/IDMIT), Université Paris-Saclay, Inserm, CEA, Fontenay-aux-Roses, France

[4]Institut Curie, PSL Research University, CNRS UMR3244, Sorbonne Université, Telomeres and Cancer, 75005 Paris, France.

[5]Centre d'Infection et d'Immunité de Lille, Inserm U1019, CNRS UMR 9017, University of Lille, CHU Lille, Institut Pasteur de Lille, 59000 Lille, France

[6]Centre de Recherche en Cancérologie de Lyon, UMR INSERM U1052/CNRS 5286, Université de Lyon, Centre Léon Bérard, Lyon, France

[7]Institute for Lung Health, Justus Liebig University, Giessen, Germany

* co-seniorized the study

Correspondence should be addressed to:

Serge Adnot, MD, PhD, Hôpital Henri Mondor, Service de Physiologie-Explorations

Fonctionnelles, 94010, Créteil, France. Tel: +33 149 812 677; Fax: +33 149 812 667; E-mail:

serge.adnot@inserm.fr

Running head: SARS-CoV2 and Cell Senescence

This article has an online data supplement, which is accessible from this issue's table of content

online at www.atsjournals.org.

To the Editor

Older age is a major risk factor for severe COVID-19 (1). Understanding the biological mechanisms linking age to the pathogenesis of COVID-19 is essential for developing preventive and therapeutic strategies. We hypothesized that cell senescence, a basic aging process that plays a pivotal role in health deterioration and diseases, particularly those targeting the lung (2), is involved in the pathogenesis of SARS-CoV-2-induced lung disease, including the development of long-lasting lung alterations. Senescent cells exhibit a stable proliferation arrest and acquire a specific senescence-associated secretory phenotype (SASP) characterized by the release of inflammatory cytokines, immune modulators, proteases, pro-fibrotic factors, and various effectors that can alter tissue organization and function (3). Senescence is triggered by a myriad of stressors that promote a DNA-damage response leading to p53-dependent upregulation of the CDK inhibitor p21 and/or expression of p16, which is used as a reliable marker of senescent cells. Cell senescence is pivotal in age-associated lung diseases, notably lung emphysema, fibrosis, and chronic obstructive pulmonary disease (2,4-6). In recent studies, SARS-CoV-2 Spike protein-1 was shown to exacerbate the SASP of human senescent cells, thereby contributing to the exuberant inflammatory response seen in severe COVID-19. Targeting senescent cells using senolytic drugs reduced mortality in old mice infected with a mouse β-coronavirus (7). To further evaluate potential links between SARS-CoV-2 infection and cell senescence, we analyzed publicly available single-cell RNA sequencing (scRNA-seq) datasets obtained using bronchoalveolar lavage fluid (BALF) cells from patients with moderate or severe-to-critical COVID-19 (8). We also monitored lung-cell senescence in SARS-CoV-2-infected macaques, which constitute a relevant model for studying human COVID-19 (9).

First, we extracted data from publicly available, BALF-cell, scRNA-seq datasets from patients with moderate or severe-to-critical COVID-19 versus healthy controls, to analyze senescence-related genes (8). In BALFs collected 10–16 days after symptom onset, mRNA of the senescence marker *CDKN2A* encoding p16 was mainly detected in epithelial cells, macrophages, and T cells, with higher levels in epithelial cells from patients with severe-to-critical disease compared to controls (Fig. 1A). Expression of the senescence markers *CDKN2A*, *CDKN1A* (encoding p21), Urokinase Plasminogen Activator Surface Receptor (uPAR), *CXCL8*, *IGFBP3*, and *GDF15* was significantly increased in epithelial ciliated and club cells from patients with severe COVID-19 compared to those with moderate disease and to healthy controls, suggesting that lung-cell senescence induction coincided with virus detection (Fig. 1B). Of note, patients with severe COVID-19 were older than those with moderate disease, whereas age was comparable between patients with moderate disease and healthy controls (Fig. 1). In single-cell datasets from another study(10), which compared same-age patients with mild vs. critical disease (supplemental Fig. S1), variations were similar, although *CDKN1A* and *CDKN2A* were less affected than in the first dataset. To further assess the extent of SARS-CoV-2-induced lung-cell senescence and the fate of senescent lung cells over time, we investigated macaques at 4 and 30 dpi, i.e., at the viral load peak and at the first negative airway-sample RT-qPCR, respectively (9). Immunohistochemical studies of lung sections at 4 dpi revealed SARS-CoV-2 antigen-stained cells, including lung endothelial cells (ECs) and parenchymal cells, as well as numerous p16- and p21-immunofluorescence-stained cells predominating at sites of alveolar damage (Fig. 2A). Cells positive for p16 were also positive for SARS-CoV-2 Spike protein-1 at 4 dpi, indicating that senescent lung cells were infected by the virus. SARS-CoV-2 antigen-stained cells were rarer at 30 dpi, whereas massive accumulation of p16- and p21-positive cells throughout the lung indicated

persistence of senescent lung cells after virus clearance (Fig. 2A). Cells stained for p16 were also stained for the DNA-damage markers γ-H2AX protein and p53-binding protein 1 at both 4 and 30 dpi (Fig. 2A).

Interestingly, the lungs at 30 dpi no longer exhibited the consolidated parenchymal areas seen at 4 dpi but showed extensive lung parenchyma remodelling, with thickening of the alveolar and pulmonary vessel walls and abundant extracellular matrix deposits as assessed by collagen staining (Fig. 2B and supplemental Fig. S2). These advanced lesions were accompanied with massive accumulation of p16- and p21-positive cells, most of which were alveolar type II cells and ECs, as shown by double-immunofluorescence staining for p16 and mucin 1 and for von Willebrand factor, respectively (Fig. 2B). Of note, most ECs stained for p16 in many lung vessels, notably those occluded by thrombi and showing intraluminal von Willebrand factor and fibrin staining. Collectively, our data constitute the first evidence of temporal and topographic relations between senescent-cell accumulation and pulmonary lesions induced by SARS-CoV-2.

Cell senescence is usually viewed as a response to chronic stressors that severely impedes healthy aging and promotes age-related noncommunicable diseases (11). Here, BALF cells from patients with severe COVID-19 expressed high levels of senescent-cell markers. This original observation was confirmed in a macaque COVID-19 model: early massive senescent lung-cell accumulation occurred in areas of severe COVID-19-related lung damage. Moreover, senescent cells persisted in the lungs over time, and many of them appeared concomitantly with the development of long-term lung alterations including remodeling of the alveolar septa and pulmonary vessels. Given the deleterious effect of cell senescence on tissue repair and inflammation, these results suggest that senescent-cell accumulation may contribute to the early lung alterations caused by SARS-CoV-2 infection and, potentially, to the post-viral lung pathology

seen in a substantial proportion of patients (12). Most ECs in thrombosed vessels were senescent, suggesting a causal relationship between EC senescence and vascular thrombosis. Thus, counteracting the cell-senescence process or eliminating senescent lung cells might lessen lung damage severity. This may be of therapeutic importance since strategies are now proposed to control senescence in various lung diseases, as well as in ARDS due to other causes (13,14). A recent study in mice showed that lung inflammation caused by a mouse β-coronavirus was markedly reduced by senolytic treatment, which also decreased mortality in old mice (7). These findings also support senescence as a major mechanism in the pathogenesis of COVID-19 and of other viral infections (15) and suggest that senescent lung-cell persistence after virus clearance may contribute to post-viral lung disease, namely emphysema or fibrosis.

Figure Legends

Figure 1. Single-cell RNAseq of cells from COVID-19 patients revealed increased expression of senescence markers in epithelial cells. (**A**) UMAP plot of cell types identified in BALFs (n=13) from the GSE145926 dataset (7). (**B**) CDKN2A mRNA was predominantly detected in epithelial cells, macrophages, and T cells. (**C**) CDKN2A expression was significantly upregulated in epithelial cells from patients with severe COVID-19. (**D**) The expression of several senescence markers (i.e., CDKN2A, CDKN1A, uPAR, CXCL8, IGFBP3, and GDF15) was significantly increased in ciliated and club cells in BALFs from patients with severe COVID-19 pneumonia compared to patients with moderate disease and to healthy controls. The statistical tests were performed using the MAST package (Finak G et al. Genome Biology 2015), and adjusted P values are reported. BALF, bronchoalveolar lavage fluid.

Figure 2A. SARS-CoV2 infection induced lung-cell senescence in cynomolgus macaques. Top. Left and middle-left panels: representative micrographs of lung tissue from non-infected animals (ni) and from animals at 4 and 30 dpi showing viral double-stranded RNA immunostaining (SARS-CoV2-J2, brown) in the parenchyma (left panel) and vessels (middle-left panel). Nuclei were stained with methyl green (blue). Middle-right and right panels: representative micrographs showing immunofluorescence of the senescence markers p16 (red) and p21 (red) in lung tissues. Green elastin autofluorescence. Nuclei were stained with DAPI (blue). Bottom. Double immunolabelling showing co-localization (pink in the merged images) of p16 (red) with SARS-CoV2 capsid protein Spike-1 (white, left panel), as well as with the DNA damage markers γH2AX (white, middle panel) and 53BP1 (white, right panel). Green elastin autofluorescence. Nuclei were stained with DAPI (blue). Bar: 50 μ. **Figure 2B**. Lung lesions associated with cell senescence. Representative micrographs of lung tissue from non-infected animals (ni) and from animals at 30

dpi showing lung lesions associated with cell senescence in the alveoli (left panel) and vessels (right panel). Top: The lung lesions identified by hematoxylin/eosin staining (alveolar thickening and vascular thrombosis) were confirmed by the Carstairs' staining showing increased collagen deposition (bright blue) and luminal fibrin (bright red) at 30 dpi. Bottom: Double immunofluorescence showing co-localization of p16-positive alveolar cells (red) with Mucin 1 (Muc1, white), a marker of type II pneumocytes (left panel), and with von Willebrand factor (vWF, white), a marker of endothelial cells (right panel). Note the intraluminal vWF staining indicating thrombosis. Green elastin autofluorescence. The nuclei were labeled with DAPI (blue). The arrows indicate thrombosis. Bar: 50 μ.

References

1. Guan WJ, Ni ZY, Hu Y, Liang WH, Ou CQ, He JX, Liu L, Shan H, Lei CL, Hui DSC, Du B, Li LJ, Zeng G, Yuen KY, Chen RC, Tang CL, Wang T, Chen PY, Xiang J, Li SY, Wang JL, Liang ZJ, Peng YX, Wei L, Liu Y, Hu YH, Peng P, Wang JM, Liu JY, Chen Z, Li G, Zheng ZJ, Qiu SQ, Luo J, Ye CJ, Zhu SY, Zhong NS, China Medical Treatment Expert Group for C. Clinical Characteristics of Coronavirus Disease 2019 in China. *N Engl J Med* 2020; 58(4):711-712.

2. Baker DJ, Wijshake T, Tchkonia T, LeBrasseur NK, Childs BG, van de Sluis B, Kirkland JL, van Deursen JM. Clearance of p16Ink4a-positive senescent cells delays ageing-associated disorders. *Nature* 2011; 479: 232-236.

3. Childs BG, Gluscevic M, Baker DJ, Laberge RM, Marquess D, Dananberg J, van Deursen JM. Senescent cells: an emerging target for diseases of ageing. *Nat Rev Drug Discov* 2017;16(10):718-735.

4. Adnot S, Amsellem V, Boyer L, Marcos E, Saker M, Houssaini A, Kebe K, Dagouassat M, Lipskaia L, Boczkowski J. Telomere Dysfunction and Cell Senescence in Chronic Lung Diseases: Therapeutic Potential. *Pharmacol Ther* 2015; 153: 125-134.

5. Amsellem V, Gary-Bobo G, Marcos E, Maitre B, Chaar V, Validire P, Stern JB, Noureddine H, Sapin E, Rideau D, Hue S, Le Corvoisier P, Le Gouvello S, Dubois-Rande JL, Boczkowski J, Adnot S. Telomere dysfunction causes sustained inflammation in chronic obstructive pulmonary disease. *Am J Respir Crit Care Med* 2011; 184: 1358-1366.

6. Kumar M, Seeger W, Voswinckel R. Senescence-associated secretory phenotype and its possible role in chronic obstructive pulmonary disease. *Am J Respir Cell Mol Biol* 2014; 51: 323-333.

7. Camell CD, Yousefzadeh MJ, Zhu Y, Langhi Prata LGP, Huggins MA, Pierson M, Zhang L, O'Kelly RD, Pirtskhalava T, Xun P, Ejima K, Xue A, Tripathi U, Machado Espindola-Netto J, Giorgadze N, Atkinson EJ, Inman CL, Johnson KO, Cholensky SH, Carlson TW, LeBrasseur NK, Khosla S, O'Sullivan MG, Allison DB, Jameson SC, Meves A, Li M, Prakash YS, Chiarella SE, Hamilton SE, Tchkonia T, Niedernhofer LJ, Kirkland JL, Robbins PD. Senolytics reduce coronavirus-related mortality in old mice. *Science* 2021;373(6552):eabe4832.

8. Liao M, Liu Y, Yuan J, Wen Y, Xu G, Zhao J, Cheng L, Li J, Wang X, Wang F, Liu L, Amit I, Zhang S, Zhang Z. Single-cell landscape of bronchoalveolar immune cells in patients with COVID-19. *Nat Med* 2020; 26: 842-844.

9. Maisonnasse P, Guedj J, Contreras V, Behillil S, Solas C, Marlin R, Naninck T, Pizzorno A, Lemaitre J, Goncalves A, Kahlaoui N, Terrier O, Fang RHT, Enouf V, Dereuddre-Bosquet N, Brisebarre A, Touret F, Chapon C, Hoen B, Lina B, Calatrava MR, van der Werf S, de Lamballerie X, Le Grand R. Hydroxychloroquine use against SARS-CoV-2 infection in non-human primates. *Nature* 2020; 585: 584-587.

10. Wauters E, Van Mol P, Garg AD, Jansen S, Van Herck Y, Vanderbeke L, Bassez A, Boeckx B, Malengier-Devlies B, Timmerman A, Van Brussel T, Van Buyten T, Schepers R, Heylen E, Dauwe D, Dooms C, Gunst J, Hermans G, Meersseman P, Testelmans D, Yserbyt J, Tejpar S, De Wever W, Matthys P, collaborators C, Neyts J, Wauters J, Qian J, Lambrechts D. Discriminating

mild from critical COVID-19 by innate and adaptive immune single-cell profiling of bronchoalveolar lavages. *Cell Res* 2021; 31: 272-290.

11. Baker DJ, Childs BG, Durik M, Wijers ME, Sieben CJ, Zhong J, R AS, Jeganathan KB, Verzosa GC, Pezeshki A, Khazaie K, Miller JD, van Deursen JM. Naturally occurring p16-positive cells shorten healthy lifespan. *Nature* 2016;530(7589):184-9.

12. Guler SA, Ebner L, Beigelman C, Bridevaux PO, Brutsche M, Clarenbach C, Garzoni C, Geiser TK, Lenoir A, Mancinetti M, Naccini B, Ott SR, Piquilloud L, Prella M, Que YA, Soccal PM, von Garnier C, Funke-Chambour M. Pulmonary function and radiological features four months after COVID-19: first results from the national prospective observational Swiss COVID-19 lung study. *Eur Respir J* 2021;57(4):2003690.

13. Chang J, Wang Y, Shao L, Laberge RM, Demaria M, Campisi J, Janakiraman K, Sharpless NE, Ding S, Feng W, Luo Y, Wang X, Aykin-Burns N, Krager K, Ponnappan U, Hauer-Jensen M, Meng A, Zhou D. Clearance of senescent cells by ABT263 rejuvenates aged hematopoietic stem cells in mice. *Nat Med* 2016; 22: 78-83.

14. Brown R, McKelvey MC, Ryan S, Creane S, Linden D, Kidney JC, McAuley DF, Taggart CC, Weldon S. The Impact of Aging in Acute Respiratory Distress Syndrome: A Clinical and Mechanistic Overview. *Front Med (Lausanne)* 2020; 7: 589553.

15. Martinez I, Garcia-Carpizo V, Guijarro T, Garcia-Gomez A, Navarro D, Aranda A, Zambrano A. Induction of DNA double-strand breaks and cellular senescence by human respiratory syncytial virus. *Virulence* 2016; 7: 427-442.
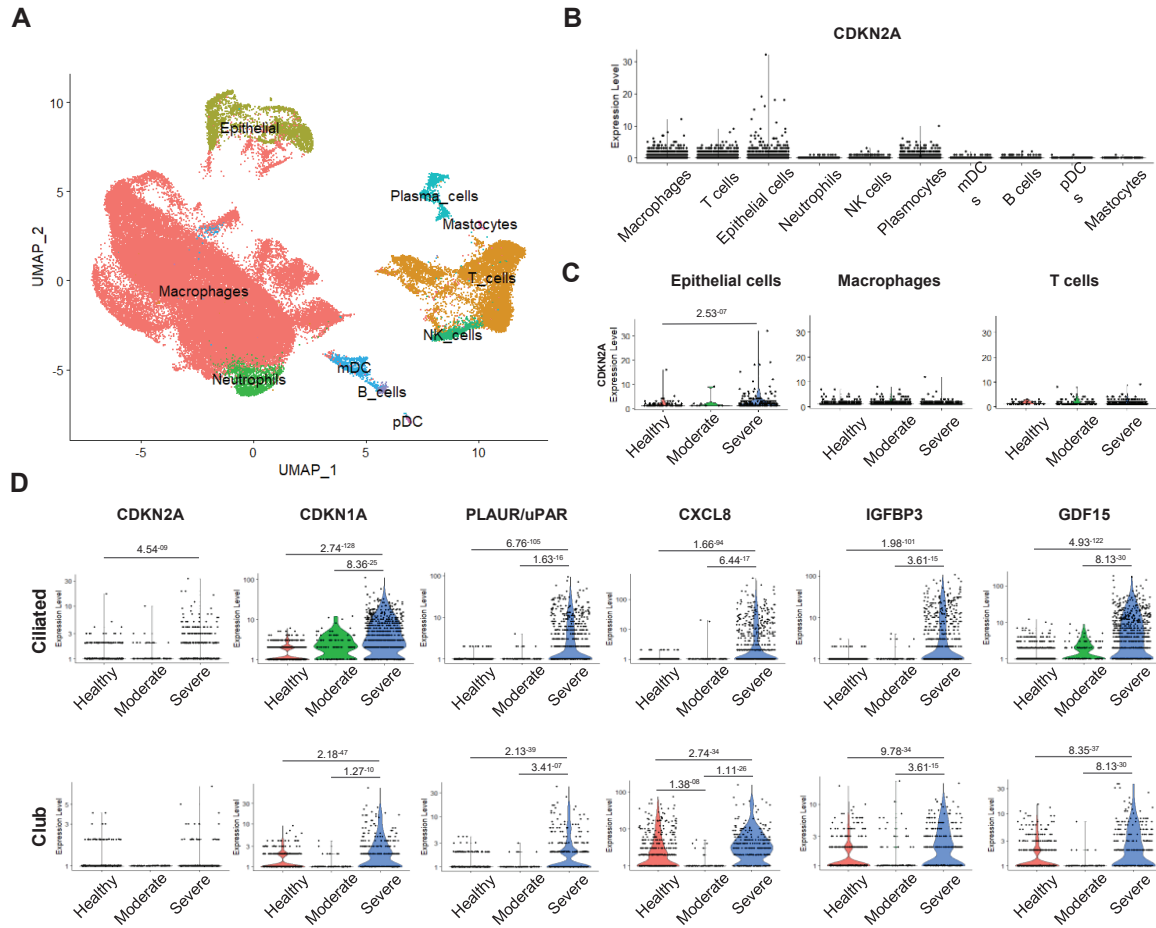
Figure 1

Figure 1. Single-cell RNAseq of cells from COVID-19 patients revealed increased expression of senescence markers in epithelial cells. (A) UMAP plot of cell types identified in BALFs (n=13) from the GSE145926 dataset (6). **(B)** CDKN2A mRNA was predominantly detected in epithelial cells, macrophages, and T cells. **(C)** CDKN2A expression was significantly upregulated in epithelial cells from patients with severe COVID-19. **(D)** The expression of several senescence markers (i.e., CDKN2A, CDKN1A, uPAR, CXCL8, IGFBP3, and GDF15) was significantly increased in ciliated and club cells in BALFs from patients with severe COVID-19 pneumonia compared to patients with moderate disease and to healthy controls. The statistical tests were performed using the MAST package (Finak G et al. Genome Biology 2015), and adjusted P values are reported. BALF, bronchoalveolar lavage fluid
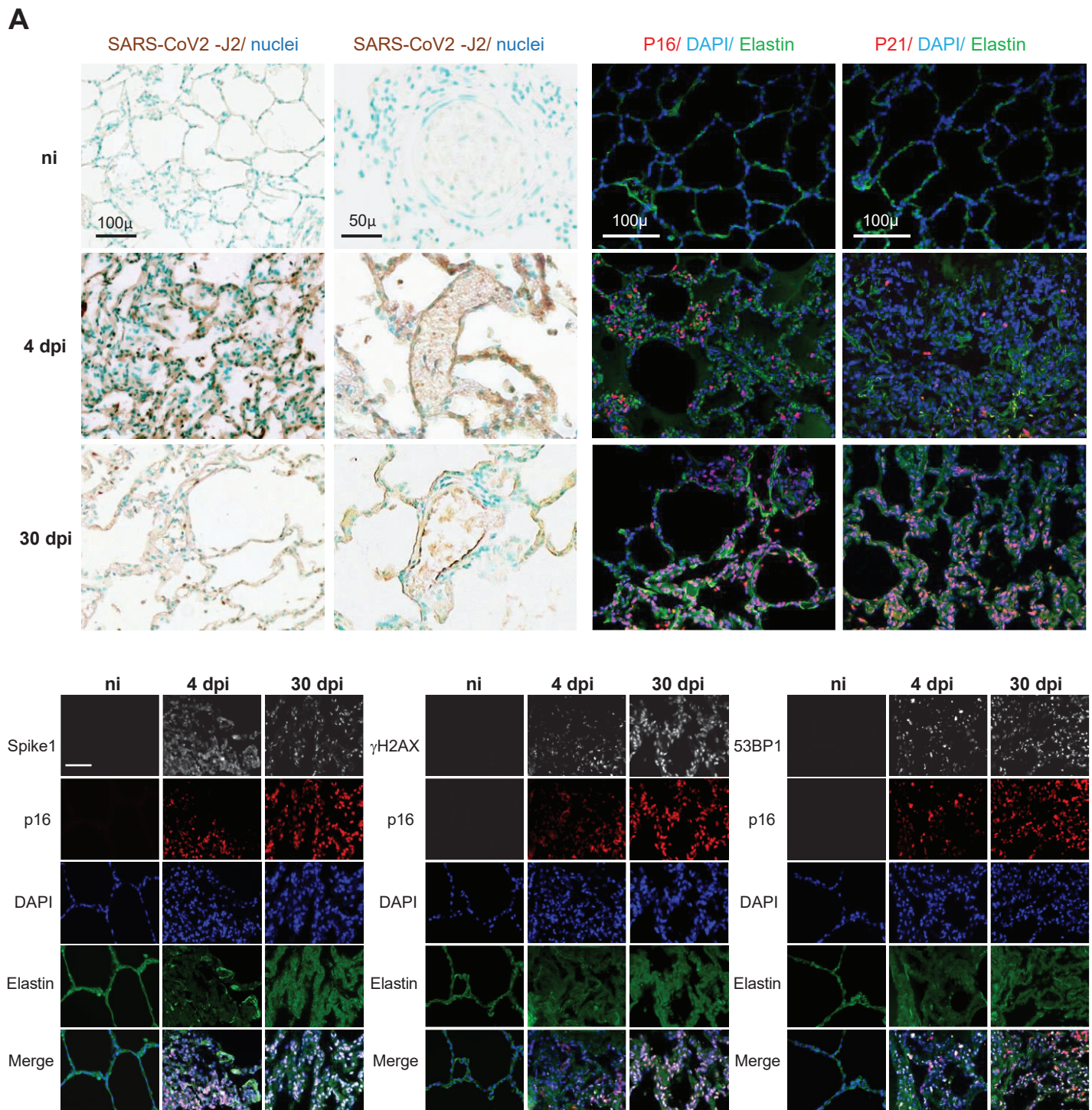
Figure 2A

A

Figure 2A. SARS-CoV2 infection induces lung cell senescence in cynomolgus macaques. Top. Left and middle left panels: representative micrographs of lung tissue from non-infected animals (ni) and from animals at 4 and 30 dpi showing viral double-stranded RNA immunostaining (SARS-CoV2-J2, brown) in parenchima (left panel) and vessels (middle left panel). Nuclei were stained with methyl green stain (blue). Middle-right and right panels: representative micrographs showing immunofluorescence of senescence markers p16 (red) and p21(red) in lung tissues. Green elastin autofluorescence. Nuclei were stained with DAPI (blue). **Bottom.** Double immunolabelling showing co-localization (pink in merged images) of p16 (red) and Sars-CoV2 capsid protein Spike1 (white, left panel) as well as with DNA damage markers γH2AX (white, middle panel) and 53BP1 (white, right panel). Green elastin autofluorescence. Nuclei were stained with DAPI (blue). Bar – 50µ.
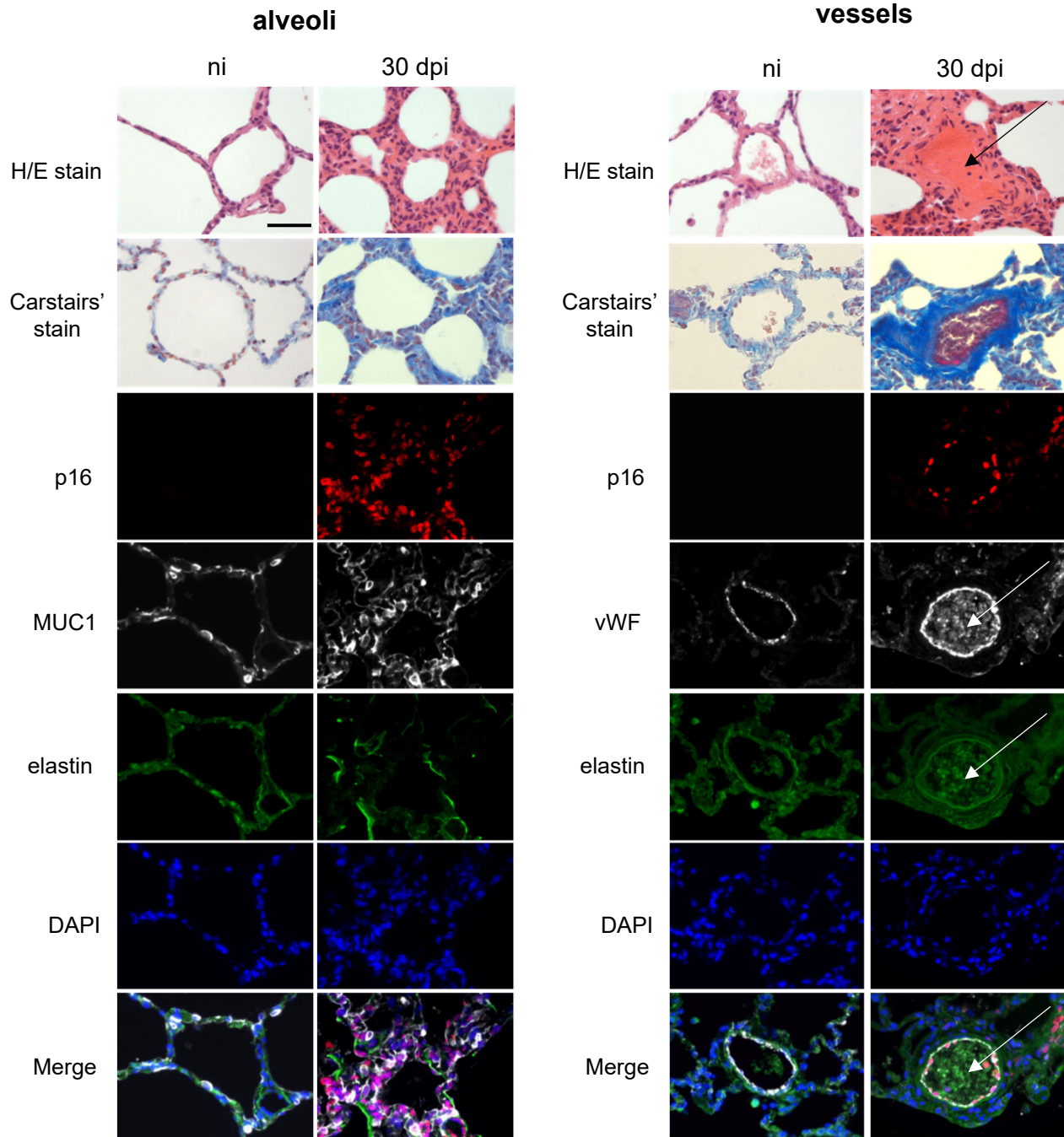
Figure 2B

B

Figure 2B. Lung lesions associated with cell senescence. Representative micrographs of lung tissue from non-infected animals (ni) and at 30 dpi showing lung lesions associated with cells senescence in alveoli (**Left panel**) and vessels (**Right panel**). **Top:** lung lesions identified by hematoxylin /eosin staining (alveolar thickening and vascular thrombosis) were confirmed by Carstairs' staining showing increased collagen deposition (bright blue) and luminal fibrin (bright red) at 30dpi. **Bottom:** Double immunofluorescence showing co-localization of p16-positive alveolar cells (red) with Mucin 1 (Muc1, white), a marker of pneumocytes type II (left panel) and with von Willebrand factor (vWF, white), a marker of endothelial cells (right panel). Note the intraluminal vWF staining indicating thrombosis. Green elastin autofluorescence. Nuclei were labeled with DAPI (blue). Arrows indicate thrombosis. Bar-50μ.

Online Data Supplement

Evidence that SARS-CoV-2 Induces Lung-Cell Senescence:

Potential Impact on COVID-19 Lung Disease

By Larissa Lipskaia, Pauline Maisonnasse, Charles Fouillade, Valentin Sencio, Quentin

Pascal, Jean-Michel Flaman, Emmanuelle Born, Arturo London-Vallejo, Roger Le Grand,

David Bernard, François Trottein and Serge Adnot

Materials and Methods

Single-cell RNA-seq analysis

We extracted data from publicly available scRNA-seq datasets obtained using cells from

bronchoalveolar lavage fluid samples cells in two separate cohorts (1,2). In the study by Liao

M et al, mean age was 36±1 years in patients with moderate disease, 62±8 years in patients

with severe or critical disease, and 29±8 years in healthy controls (1). Mean ages in patients

with moderate or severe disease studied by Wauters E et al. were similar (2). Count matrices

were initially processed by the authors as described in the original studies (1,2). Briefly, raw

matrices were loaded in Seurat, and low-quality cells were removed by conventional quality

controls. Each sample/patient was integrated using canonical correlation analysis (CCA) and,

after principal component analysis and graph-based clustering, each cluster was annotated

based on the expression of canonical markers. Differential gene-expression analysis was

performed using Model-based Analysis of Single-cell Transcriptomics (MAST) (3).

Expression of senescence markers was visualized using the VlnPlot function available in

Seurat.

Animal studies

Ethics and biosafety statement

Cynomolgus macaques (*M. fascicularis*) aged 37–40 months and originating from Mauritian AAALAC-certified breeding centers were used as previously described (4). All macaques were housed in IDMIT infrastructure facilities (CEA, Fontenay-aux-Roses), under BSL-2 and BSL-3 containment when necessary (animal facility authorization D92-032-02, Prefecture des Hauts de Seine, France) and in compliance with European Directive 2010/63/EU, French regulations, and the Standards for Humane Care and Use of Laboratory Animals developed by the Office for Laboratory Animal Welfare (OLAW, assurance number A5826-01, Bethesda, MD). The protocols were approved by the institutional review board *Comité d'Ethique en Expérimentation Animale du Commissariat à l'Energie Atomique et aux Energies Alternatives* (CEtEA 44) under statement number A20-011. The study was authorized by the French Research, Innovation, and Education Ministry under registration number APAFIS#24434-2020030216532863v1.

Study design

Challenged macaques were exposed to a total dose of 10^6 PFU of SARS-CoV-2 clinical isolate (BetaCoV/France/IDF/0372/2020) by combined intranasal and intratracheal administration (day 0), using atropine (0.04 mg·kg^{-1}) for premedication and ketamine (5 mg·kg^{-1}) with medetomidine (0.042 mgkg^{-1}) for anesthesia (3). The macaques were observed daily. Clinical examinations were performed at baseline then daily for one week and finally twice weekly, with anesthesia using ketamine (5 mg·kg^{-1}) and medetomidine (0.042 mgkg^{-1}). Body weight, rectal temperature, respiration rate, heart rate, and oxygen saturation were recorded. Blood samples and nasopharyngeal, tracheal, and rectal swabs were collected. The macaques were humanely euthanized 4 and 30 days post infection (dpi) using

18.2 mg·kg^{-1} of pentobarbital sodium intravenously under tiletamine (4 mg·kg^{-1}) and zolazepam (4 mg·kg^{-1}) anesthesia. Lung samples were collected at necropsy

Histopathology and immunohistochemistry

For the histopathology studies, autopsy specimens were formalin-fixed and paraffin-embedded following standard procedures. Paraffin-embedded sections were deparaffinized using xylene and a graded series of ethanol dilutions. Tissue sections 5-µM in thickness were stained with hematoxylin/eosin or with the Carstairs' Method for Fibrin & Platelets (EMS, Catalog#26381-Series).

For immunohistochemistry, antigens were retrieved by incubation in citrate buffer (0.01 M, pH 6) at 90°C for 15 minutes. Endogenous peroxidase activity was blocked with 3% H$_2$O$_2$ and 10% methanol in PBS for 10 minutes. Permeabilization was achieved using 0.1% Triton X-100 in PBS for 10 min.
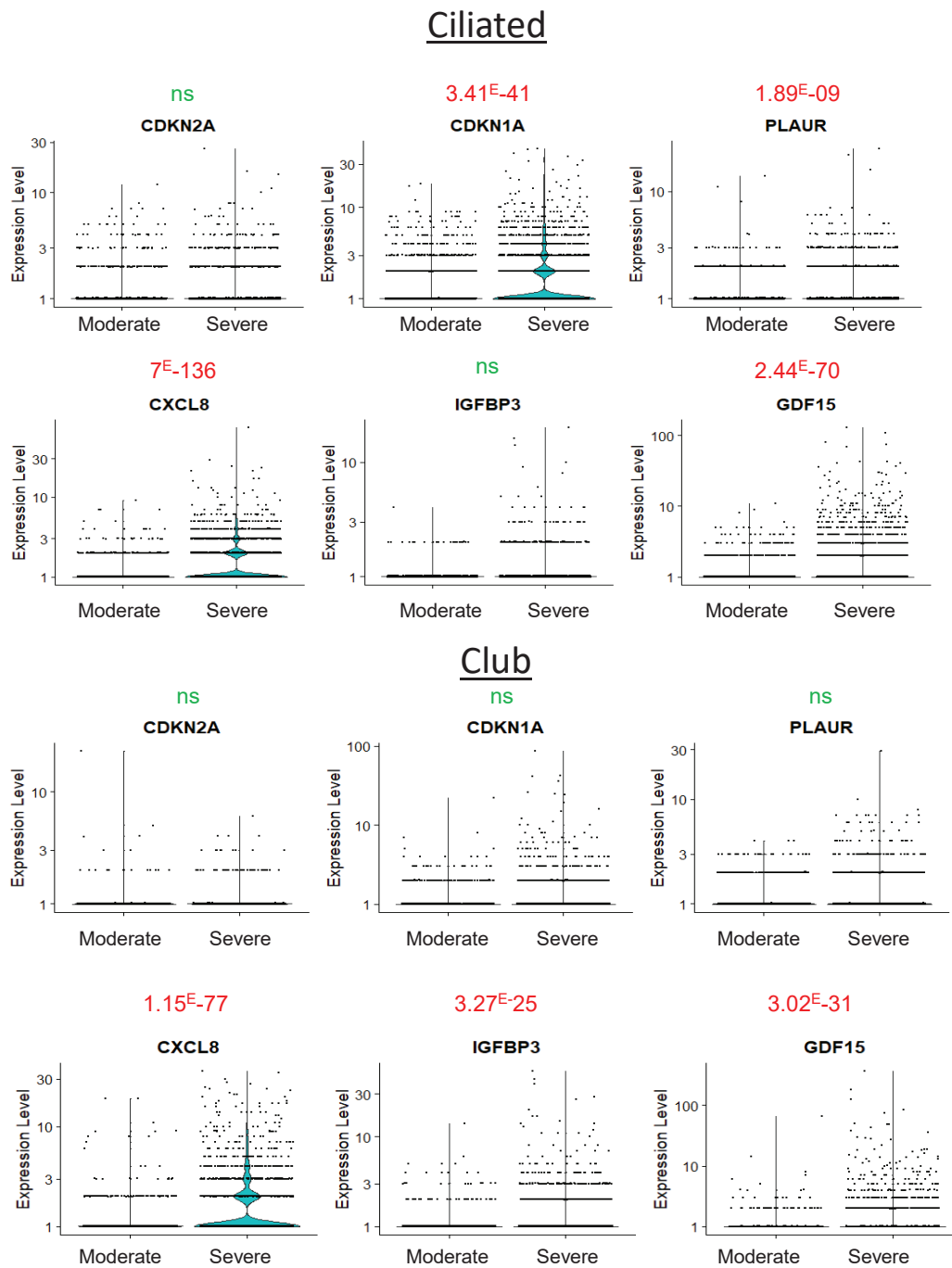
Lung immunohistochemical analyses were performed using N-Histofine Simple Stain MAX PO (H1410I, Nichirei Bioscience Inc., Tokyo, Japan) with anti-dsRNA-J2 used as the primary anti-SARS-Cov-2 antibody (1:1000, RNT-SCI-10010200, Jena Bioscience, Jena, Germany). Co-immunolocalization of the SARS-CoV-2 capsid protein Spike-1 with p16 was assessed using the AlexaFluor^{TM} 555 Tyramide SuperBoost^{TM} Kit (B40923, Invitrogen, Waltham, MA). Amplification was applied for the anti-Spike-1 antibody (1:1000, GTX 635654, GeneTex, Irvine, CA) and the second primary antibody was anti-p16 (1:200, ab54210, Abcam, Cambridge, UK). The primary antibodies for standard immunofluorescence were anti-p16 (1:200, ab54210, Abcam), anti-p21 (1:200, ABIN6939038, antibodies-online.com, GmbH, Karlsruhe, Germany), anti-mucin1 (1:200, MUC1 ab109185, Abcam); anti-von Willebrand Factor (vWF) (1:200, ab6994, Abcam), anti-53BP1 (1:200, NB100-304, Novusbio, Littleton, CO), and anti-γ-H2AX (1:200, MA5-33062, RRID AB-2810155, Thermo Fisher

Scientific, Waltham, MA). The secondary antibodies were anti-rabbit Alexa Fluor® 555 and anti-mouse Alexa Fluor® 660 (1:400, Invitrogen). The nuclei were stained with Hoechst (1 µL/mL, Cell Signaling Technology, Danvers, MA). Fluorescence was measured using an Axioimager M2 Imaging microscope (Zeiss, Oberkochen, Germany) and quantified on digital photographs using Image J software (imagej.nih.gov/ij/).

References

1. Liao M, Liu Y, Yuan J, Wen Y, Xu G, Zhao J, Cheng L, Li J, Wang X, Wang F, Liu L, Amit I, Zhang S, Zhang Z. Single-cell landscape of bronchoalveolar immune cells in patients with COVID-19. *Nat Med* 2020; 26: 842-844.

2. Wauters E, Van Mol P, Garg AD, Jansen S, Van Herck Y, Vanderbeke L, Bassez A, Boeckx B, Malengier-Devlies B, Timmerman A, Van Brussel T, Van Buyten T, Schepers R, Heylen E, Dauwe D, Dooms C, Gunst J, Hermans G, Meersseman P, Testelmans D, Yserbyt J, Tejpar S, De Wever W, Matthys P, collaborators C, Neyts J, Wauters J, Qian J, Lambrechts D. Discriminating mild from critical COVID-19 by innate and adaptive immune single-cell profiling of bronchoalveolar lavages. *Cell Res* 2021; 31: 272-290.

3. Finak G, McDavid A, Yajima M, Deng J, Gersuk V, Shalek AK, Slichter CK, Miller HW, McElrath MJ, Prlic M, Linsley PS, Gottardo R. MAST: a flexible statistical framework for assessing transcriptional changes and characterizing heterogeneity in single-cell RNA sequencing data. *Genome Biol* 2015; 16: 278.

4. Maisonnasse P, Guedj J, Contreras V, Behillil S, Solas C, Marlin R, Naninck T, Pizzorno A, Lemaitre J, Goncalves A, Kahlaoui N, Terrier O, Fang RHT, Enouf V, Dereuddre-Bosquet N, Brisebarre A, Touret F, Chapon C, Hoen B, Lina B, Calatrava MR, van der Werf S, de Lamballerie X, Le Grand R. Hydroxychloroquine use against SARS-CoV-2 infection in non-human primates. *Nature* 2020; 585: 584-587.

Supplemental figure 1

Ciliated

(violin plots for CDKN2A [ns], CDKN1A [3.41^{E}-41], PLAUR [1.89^{E}-09], CXCL8 [7^{E}-136], IGFBP3 [ns], GDF15 [2.44^{E}-70] comparing Moderate vs Severe)

Club

(violin plots for CDKN2A [ns], CDKN1A [ns], PLAUR [ns], CXCL8 [1.15^{E}-77], IGFBP3 [3.27^{E}-25], GDF15 [3.02^{E}-31] comparing Moderate vs Severe)

Supplemental Figure 1. Single cell RNAseq of material from patients with COVID-19 (n=22) in the EGAS00001004717 dataset (Wauters et al., 2021) **revealed increased expression of senescence markers in epithelial cells**. **(D)** Expression of several senescence markers (i.e., CDKN1A, PLAUR, CXCL8, IGFBP3, and GDF15) is significantly increased in ciliated cells (**Top Panel**) and club cells (**Bottom Panel**) in BALFs from patients with severe COVID-19 pneumonia compared to patients with moderate disease. The statistical tests were performed using the MAST package (Finak G. et al., Genome Biology 2015) and adjusted *P* values are reported.

Supplemental Figure 2.

Hematoxylin/eosin staining

ni   30 dpi

Carstairs' staining

ni   30 dpi

500µ
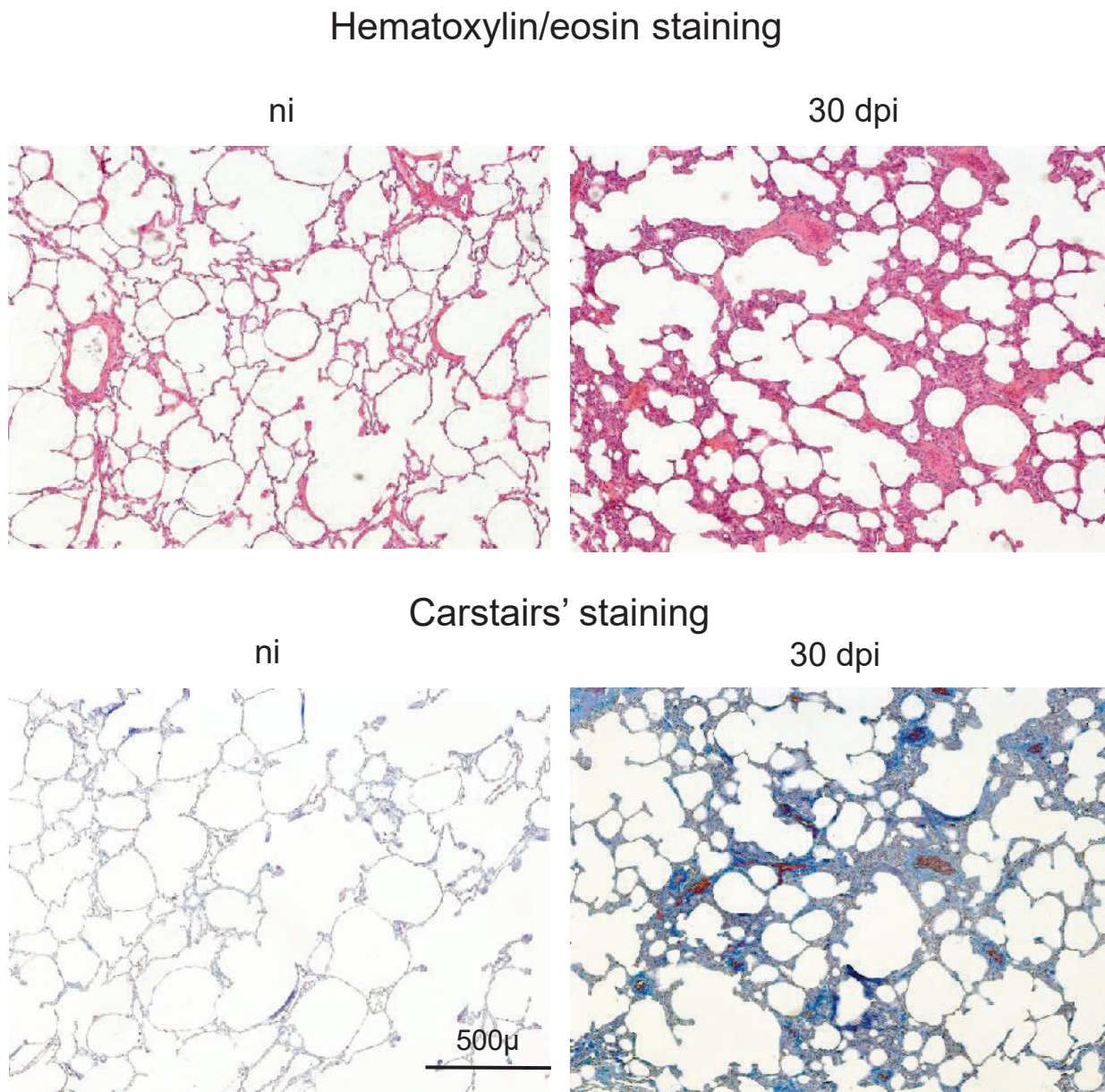
Supplemental Figure S2. **Post-Covid lung lesions**. Hematoxylin /eosin staining (**Top Panel**) and Carstairs' staining (**Bottom Panel**) in non-infected animals (ni) and at 30 dpi. Hematoxylin /eosin staining   showed alveolar thickening and Carstairs' staining evidencing increased collagen deposition (bright blue) and luminal fibrin (bright red) at 30 dpi. These staining pulmonary fibrosis and vascular thrombosis, respectively.